

Total oxidation of methanol on Cu(110): a density functional theory study

Sung Sakong* and Axel Groß

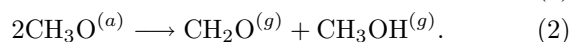
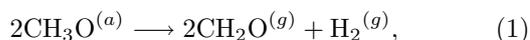
Institut für Theoretische Chemie, Universität Ulm, Albert-Einstein-Allee 11, 89081 Ulm/Germany

The partial and total oxidation of methanol on clean and oxygen-precovered Cu(110) has been studied by periodic density functional theory calculations within the generalized gradient approximation. Reaction paths including the geometry and the energetics of several reaction intermediates and the activation barriers between them have been determined thus creating a complete scheme for the methanol oxidation on copper. The calculations demonstrate that the specific structure of oxygen on copper plays an important role in both the partial and the total oxidation of methanol. For lower oxygen concentration on the surface, the partial oxidation of methanol to formaldehyde is promoted by the presence of oxygen on the surface through the removal of hydrogen in the form of water which prevents the recombinative desorption of methanol. At larger oxygen concentrations, the presence of isolated oxygen atoms reduces the C-H bond breaking barrier of adsorbed methoxy considerably thus accelerating the formation of formaldehyde. Furthermore, oxygen also promotes the formation of dioxymethylene from formaldehyde which then easily decays to formate. Formate is the most stable reaction intermediate in the total oxidation. Thus the formate decomposition represents the rate-limiting step in the total oxidation of methanol on copper.

I. INTRODUCTION

Methanol is the smallest alcohol molecule and a technologically important molecule whose synthesis and oxidation is catalyzed by, e.g., copper. In spite of the simplicity of methanol, still its oxidation process on catalytic surfaces exhibits a surprisingly large complexity with several different possible reaction routes. According to temperature programmed desorption (TPD) experiments [1, 2] using isotope labeling, on copper the methanol oxidation starts with its decomposition into methoxy (CH_3O) and hydrogen, in contrast to Pt-based catalysts on which the O-H and the C-H bond scission pathways have comparable activation barriers [3].

The next methanol oxidation step on copper, namely the decomposition of methoxy into formaldehyde (CH_2O) and hydrogen, is known to be efficiently promoted by the presence of oxygen on the surface [1, 4]. However, for low oxygen concentrations this effect is rather indirect by removing the hydrogen atoms on the surface in the form of water [1, 5]. Thus the recombinative desorption path of methoxy and hydrogen as methanol is no longer available, so that only the following reactions are possible:



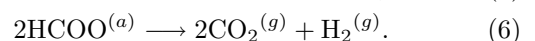
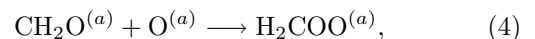
These reactions occur on clean Cu(110) at temperatures above 370 K [4, 6, 7]. At these temperatures, the produced formaldehyde is immediately removed from the surface because of its small binding energy.

Thus, this reaction route does not lead to the total oxidation of methanol. Instead, either a formaldehyde

formation channel is needed that is active at lower temperatures so that formaldehyde does not desorb directly after its formation, or active sites are required that promote the further oxidation of formaldehyde. In fact, the total oxidation of methanol to carbon dioxide is only possible under specific reaction conditions associated with a high oxygen coverage [1, 4, 8] which open up the following reaction channel:



In many studies, formate (HCOO) has been presumed to be a reaction intermediate in the full oxidation [1, 2, 9–11]. One possible route for the formate formation is that first formaldehyde and surface oxygen interact to create dioxymethylene (H_2COO) which converts to formate at low temperature [12, 13]. This results in the following tentative reaction scheme [11, 13, 14] for the CO_2 formation:



Since formate is a very stable reaction intermediate, the last reaction (6) represents the rate limiting step in the methanol oxidation which occurs at 470 K on Cu(110) [1].

These facts show that the precise state and concentration of oxygen on the copper surface play an important role in the oxidation of methanol. At room temperature, oxygen exposure induces a surface rearrangement into an *added row* $p(2 \times 1)$ reconstruction on Cu(110) [15, 16]. This structure consists of CuO chains that form a stripe phase with a periodicity of 60 Å leading to a nominal oxygen coverage of 0.25 ML [17, 18]. Thus, the surface can be divided into clean areas, oxygen islands and the edges of the oxygen islands. According to scanning tunneling microscopy (STM) studies, the oxygen atoms in the islands are catalytically inactive. Active oxygen atoms are

*New address: Fachbereich Physik, Universität Duisburg-Essen, 47048 Duisburg/Germany

rather those at the [001] edge of oxygen islands or at isolated oxygen sites [19, 20]. Unfortunately, the realistic theoretical description of such terminal sites requires a significant computational effort.

We have recently addressed the partial oxidation of methanol on clean and oxygen-covered Cu surface by periodic density functional theory (DFT) calculations and kinetic Monte Carlo simulations [5–7]. For the sake of computational efficiency, we had chosen isolated oxygen atoms at the Cu pseudo hcp hollow sites in a (2×2) structure as an active site model for the oxygen-covered Cu(110) surface. Since there are strong geometric and electronic similarities with the terminal oxygen sites at the CuO chains, this model gives a satisfactory semi-quantitative description of the partial oxidation of methanol on oxygen-covered Cu(110) [5].

We have now used this active site model in order to extend the study to the total oxidation of methanol on Cu(110). In addition, we have recalculated the methanol pathways towards partial oxidation using a better description of the electronic core states. Furthermore, based on the results of the kinetic Monte Carlo simulations [6, 7] we had identified some discrepancies between calculated and experimentally derived barrier heights in the methanol oxidation. In order to elucidate the reasons for these discrepancies we have considered selected processes using realistic reconstructed surface geometries for oxygen-covered Cu(110). Thus we are able to provide a consistent picture of the total oxidation of methanol on Cu(110) demonstrating the importance of the specific oxygen structure on copper for the single reaction steps.

II. THEORETICAL METHODS

Periodic DFT calculations have been performed using the Vienna *ab-initio* simulation package (VASP) [21]. The exchange-correlation effects have been described within the generalized gradient approximation (GGA) through the Perdew-Burke-Ernzerhof (PBE) functional [22]. The ionic cores are represented by projector augmented wave (PAW) potentials [23] as constructed by Kresse and Joubert [24]. The plane wave basis has been expanded up to a cutoff energy of 400 eV.

The Cu substrates are modeled by slabs of five layers that are separated by a 12 Å vacuum. In all calculations, the two uppermost Cu layers are fully relaxed. Most results reported here have been obtained for 2×2 and 3×3 surface unit cells for which we have used Monkhorst-Pack \mathbf{k} -point sets of 7×7 and 5×5 , respectively. In order to simulate the [001] edge of the $p(2 \times 1)$ oxygen islands in the added row reconstruction (see Fig. 1), a 2×6 unit cell was chosen, resulting in 11 Å of the CuO chain along the [001] direction separated by 10 Å of clean Cu(110). To study adsorption at the $[1\bar{1}0]$ edge of the CuO chain an infinite CuO chain within a 3×2 geometry was chosen. The transition states are determined with the nudged elastic band (NEB) method that has been developed by

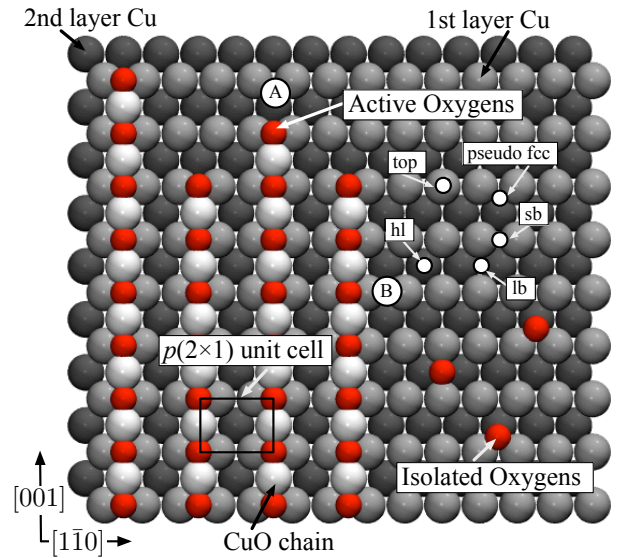


FIG. 1: Schematic presentation of the oxygen-covered Cu(110) surface. Oxygen induces a $p(2 \times 1)$ added-row reconstruction consisting of CuO chains that form a stripe phase. The terminal oxygen species active for methanol oxidation are located at the [001] edge of the chains.

Jónsson *et al.* [25, 26] with the two uppermost Cu layers allowed to relax during the transition state search.

The adsorption energies are defined with respect to the isolated substrate and the molecules in the gas phase. Negative signs represent an attractive interaction. Note that some of the binding and activation energies reported in this work differ by up to 0.2 eV with respect to our previous study [5]. There are two reasons for the discrepancies. A significant part of the changes comes from the fact that in our previous study we have kept the substrate fixed during the transition state search. Additionally, we have now used the PAW method instead of ultrasoft pseudopotentials (USPP) [27] to treat the effect of the core electrons. They are better described in the PAW method which corresponds to an all-electron method [23]. This is particularly true for the treatment of oxygen for which for example the PAW result of the O_2 binding energy is much closer to all-electron results than the USPP result [28]. The geometries of the reaction intermediates and the transition states, however, are hardly affected by this choice.

III. RESULTS

A. Structure of the oxygen-covered Cu(110) surface

The oxygen-induced $p(2 \times 1)$ added-row reconstruction of Cu(110) is illustrated in Fig. 1. It consists of CuO chains in [001] direction that form a stripe phase with long and short edges in $[1\bar{1}0]$ and [001] directions, re-

spectively. The short edges are terminated by oxygen atoms that are active for methanol oxidation [19, 20]. According to the DFT calculations, oxygen atoms at the terminal positions of the chains are 0.5 eV more strongly bound than isolated oxygen atoms on Cu(110), although both oxygen atoms are effectively three-fold coordinated (see Fig. 1). This is mainly caused by the lower coordination of the Cu atoms in the CuO chains of the added row reconstruction. The large energy gain makes the O-terminated CuO chains in fact more stable than the Cu-terminated ones. Using the definition

$$E_{\text{form}} = \frac{E_{\text{tot}} - (E_{\text{Cu}(110)} + n_{\text{Cu}}E_{\text{Cu}}^{\text{bulk}} + n_{\text{O}}E_{\frac{1}{2}\text{O}_2}^{\text{gas}})}{n_{\text{Cu}} + n_{\text{O}}}, \quad (7)$$

in order to determine the formation energy of the CuO chains per chain atom, where n_{Cu} and n_{O} are the number of Cu and oxygen atoms, respectively, in the CuO chain, we find that the oxygen-terminated CuO chain is 0.51 eV more favorable than the copper-terminated chain which is in a good agreement with the observations in STM experiments [20].

Before methanol exposure, the oxygen islands are elongated along the [001] direction and thus the number of available active oxygen atoms is low. However, in an autocatalytic manner the methanol oxidation leads to the formation of defect in the CuO chains of the oxygen islands which increases the number of active oxygen atoms [19].

These active terminal oxygen atoms are located at pseudo hcp hollow sites. As already mentioned, there are large geometric and thus electronic similarities between the terminal oxygen atoms and isolated oxygen atoms at their most stable site which also corresponds to a pseudo threefold hollow site (see Fig. 1). Therefore, we will use the isolated oxygen atoms as an effective model for the terminal oxygen atoms in order to assess the role of oxygen in the methanol oxidation on Cu(110).

Still there are significant differences between these two sites caused by second-nearest neighbor effects. We have probed the activity at the [001] edge by hydroxyl formation. We have assumed that atomic hydrogen approaches the oxygen and forms a hydroxyl (OH). The hydroxyl formation is associated with an energy gain of -0.56 eV at the terminal oxygen sites, whereas this gain is -1.03 eV at the isolated oxygen atoms (note that more negative energies corresponds to more favorable sites). Clearly, the activity of the isolated atomic oxygen is stronger than those of the terminal atoms which can be easily understood by the fact that the terminal oxygen atoms are more strongly bound which makes them more inert. In fact, addressing the properties of these isolated oxygen atoms is worthwhile in its own right since such an active species has been postulated [11] in order to explain the higher activity toward formate production in oxygen and methanol co-dosing experiments [11] or under steady state conditions [29] as compared to oxygen pre-dosing experiments. Our calculations show that these isolated oxygen atoms are indeed crucial in order to understand the total oxidation of methanol on Cu(110).

B. Properties of the reaction intermediates in the methanol oxidation on Cu(110)

The adsorption properties of the reaction intermediates in the methanol oxidation at various sites have been calculated on clean and oxygen-precovered Cu surfaces. The data for clean Cu(110) are listed in Table I. The calculations show that methanol is only weakly bound to clean Cu(110). Such a state has also been identified in TPD experiments [30]. However, our recent kinetic Monte Carlo (kMC) simulations [6, 7] and other TPD experiments [1] indicated the existence of a more strongly bound methanol species on oxygen-covered Cu(110). We have therefore performed an extensive search for further methanol adsorption configurations on clean and oxygen precovered Cu surfaces. In Fig. 2, methanol adsorption energies are plotted for various configurations in terms of the distance between methanol and nearest Cu atom. There is a broad range of adsorption energies from -0.05 to -0.77 eV. Methanol adsorbs only weakly on clean Cu and above the oxygen islands formed by the $p(2 \times 1)$ added-row reconstruction. Furthermore, the decomposition of methanol via hydroxyl bond breaking is endothermic by 1.29 eV in the added-row reconstruction. This indicates that the $p(2 \times 1)$ oxygen areas themselves are inactive as far as the methanol oxidation is concerned which has also been observed in the experiment [19, 20].

The interaction of methanol with isolated oxygen atoms, on the other hand, leads to the spontaneous hy-

Reaction intermediate	Adsorption configuration	E_{ads} (eV)	$h_{\text{Cu-O}}$ (Å)	$d_{\text{Cu-O}}$ (Å)	Orientation
CH ₃ OH	O _t -H _{lb}	-0.34	2.09	2.16	tilted
	O _t -H _{lb}	-0.26	2.09	2.16	
	O _{sb} -H _{hl}	-0.26	1.88	2.36	
CH ₂ O	η^2	-0.46	1.20	2.03	
	physisorption	-0.06	2.88	-	
CH ₃ O	O _{sb}	-2.94	1.44	1.96	tilted
	O _{lb}	-2.54	1.17	2.04	
	O _{lb}	-2.56	1.18	2.05	
H ₂ COO	O _{sb} -C _{hl} -O _{sb}	-0.61	1.30	1.97	along [001]
	O _t -C _{lb} -O _t	+0.51	1.75	1.84	along [001]
	O _{lb} -C _{hl} -O _{lb}	-0.09	1.20	2.05	along [110]
	O _t -C _{sb} -O _t	+0.60	1.85	1.85	along [110]
HCOO	O _t -C _{sb} -O _t	-3.37	1.98	1.96	along [110]
	O _t -C _{lb} -O _t	-3.31	1.87	1.97	along [001]
CO ₂	physisorption	-0.06	3.09	-	
H ₂ O	O _{sb}	-0.20	1.97	2.49	

TABLE I: Adsorption properties of reaction intermediates on clean Cu(110). The adsorption configurations are denoted by the (110) high symmetry positions that are closest to the atoms of the methanol molecule that are directly bound to the Cu substrate. For the weakly bound species denoted by physisorption the adsorption energy is practically independent of the lateral position. Dioxymethylene is not stable in the gas phase, therefore the adsorption energy is given with respect to the energy of the free CO₂ and H₂ molecule, i.e. $E_{\text{ref}} = E[\text{Cu}(110)] + E[\text{CO}_2^{(g)}] + E[\text{H}_2^{(g)}]$.

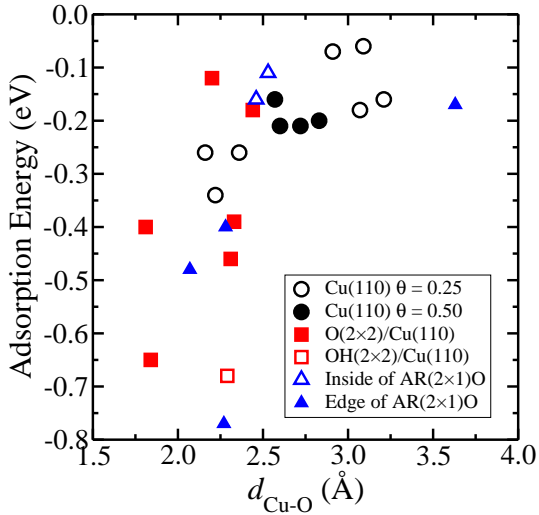


FIG. 2: Adsorption energy of methanol as a function of the distance between the methanol oxygen atom and the nearest Cu atom. The energies are defined with respect to the isolated substrate and methanol in the gas phase. The methanol coverage for the clean Cu(110) substrate is $\theta_{\text{CH}_3\text{OH}} = 0.25$ and 0.5, whereas it is 0.25 for the oxygen- and hydroxyl covered Cu(110) surface within a $p(2 \times 2)$ geometry. For the added row reconstruction (AR), there is one methanol molecule in the corresponding unit cells that are described in section II.

droxyl bond (OH) breaking [5] resulting in methoxy and hydroxyl on the surface. Isolated surface hydroxyl is less active than surface oxygen in the OH bond breaking, but it still interacts rather attractively with methanol, as Fig. 2 shows.

Hence isolated oxygen atoms cannot be the source for the more strongly bound methanol species since they are too reactive. In fact, the active oxygen atoms at the [001] edges of the CuO chains are bound with an intermediate strength so that they can attract methanol considerably, but do not induce a spontaneous methanol decomposition. At the site A indicated in Fig. 1 the methanol adsorption energy is enlarged to -0.77 eV. These sites seem to be good candidates for the adsorbed methanol species in the presence of oxygen on Cu(110) with an experimentally derived binding energy of 0.65 eV [1].

Along the $[1\bar{1}0]$ edge of the CuO chains, the oxygen atoms are more tightly bound than at the [001] edge. These less active oxygens interact still attractively with methanol in neighboring clean surface cell (site B in Fig. 1) increasing the adsorption energy to -0.48 eV. The methanol-oxygen interaction is in fact so strong that it induces a change of the Cu-O distance from its equilibrium value of 1.83 Å to 1.88 Å.

Thus, various more strongly bound methanol species exist at the edge sites of the $p(2 \times 1)$ oxygen islands. These variety could be an explanation for the discrepancy between the broad methanol desorption peak found in the TPD experiments [1] and the narrow methanol desorption peak in kMC simulations [6, 7]. It furthermore con-

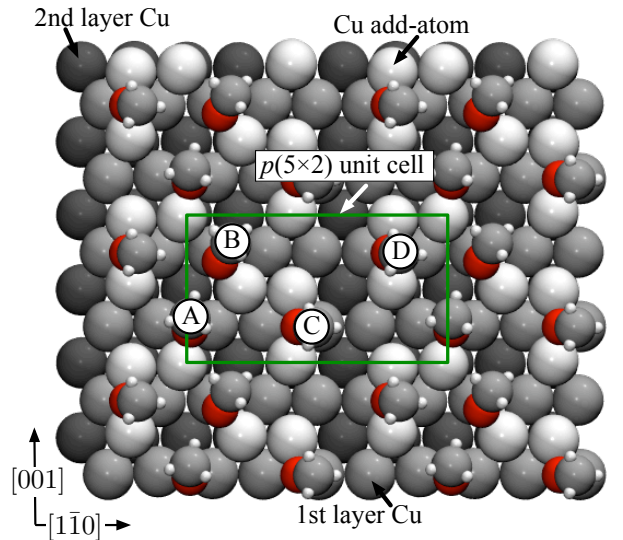


FIG. 3: Calculated $p(5 \times 2)$ methoxy structure on Cu(110) based on structural models proposed by Leibslle et al. [11, 31].

firms the need to consider realistic surface oxygen structures for a quantitative comparison between theory and experiment.

Using STM, Leibslle et al. [31, 32] have shown that the conversion of methanol to methoxy is associated with the removal of the terminal oxygen atoms resulting in the shrinking of the $p(2 \times 1)$ oxygen islands. At the same time, a $p(5 \times 2)$ methoxy-induced reconstruction is formed. Based on STM and low-energy electron diffraction (LEED) data, structural models of the $p(5 \times 2)$ reconstruction have been proposed that incorporate added Cu atoms from the CuO-chains [11, 31]. Based on these suggestions we have looked for the energy-minimum structure which is illustrated in Fig. 3. After the oxygen removal, the Cu add-atoms create an energetically stable $p(5 \times 2)$ structure with the methoxy intermediates located at low symmetry positions, namely at a pseudo hcp site (site A in Fig. 3), at an edge site (B) and at long bridge positions (C and D). The mean adsorption energy is -2.90 eV per methoxy molecule which is comparable to the most stable methoxy configuration at the short bridge site on clean Cu(110).

Among all the reaction intermediates in the methanol oxidation on Cu, formate (HCOO) is the most stable one. It is bound through two oxygen atoms that are located above two neighboring Cu atoms with the carbon atom at the bridge site [33]. Both orientations involving the short-bridge position along the $[1\bar{1}0]$ direction along the close-packed copper rows and the long-bridge position along [001] show similar adsorption energies, however, when the O-C-O bond is oriented along the Cu rows of the (110) surface in $[1\bar{1}0]$ direction, it is slightly more stable than for the perpendicular orientation along [001] across the Cu rows. Dioxymethylene (H_2COO) also adsorbs through its two oxygen atoms,

however, these oxygen atoms are rather located above the Cu short-bridge sites, and in contrast to the formate dioxyethylene prefers to be oriented perpendicular to the Cu rows along the [001] direction. It should be noted that dioxyethylene is not stable in the gas-phase but rather decomposes into CO_2 and H_2 . Therefore the adsorption energy of dioxyethylene is given with respect to these stable molecules, and thus it also contains the energy cost of the dioxyethylene formation.

The diffusion barriers of selected intermediates on clean Cu(110) are listed in Table II. Because of the anisotropy of the (110) surface, the diffusion barriers for propagation along the troughs in $[\bar{1}\bar{1}0]$ direction differ from the barriers for diffusion perpendicular to the rows which enhances the corrugation of the surface compared to the close-packed Cu surfaces [34]. In general, the diffusion along the direction of the close-packed rows is much more facile than the diffusion across the troughs of the (110) surface. For hydrogen, the situation is a little bit more complex. The diffusion barrier for the jump from the pseudo fcc site across the short-bridge to the adjacent pseudo fcc site along the [001] direction is only 0.04 eV. However, a further movement to the next pseudo fcc site at the other side of the trough requires a motion via the long-bridge site which is hindered by a barrier of 0.17 eV (see Table II). So effectively the diffusion barrier for diffusion in both the [001] and the $[\bar{1}\bar{1}0]$ direction is hindered by the same barrier of 0.17 eV. In comparison, on Cu(100) the hydrogen diffusion barrier is only 0.08 eV [35].

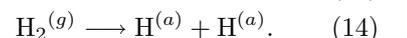
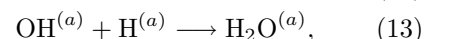
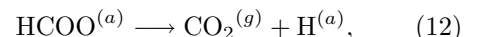
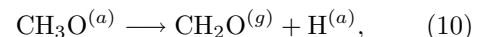
Methanol can diffuse practically freely in $[\bar{1}\bar{1}0]$ direction, whereas its diffusion in [001] direction is hindered by a barrier of 0.27 eV. The methoxy diffusion along the Cu rows is also rather facile (diffusion barrier 0.08 eV), whereas perpendicular to the rows the barrier is 0.48 eV. It should be noted that methoxy forms a $c(2 \times 2)$ struc-

ture which is 50 meV more stable per molecule than the $p(2 \times 2)$ according to our calculations. On the other hand, diffusion in this densely packed methoxy islands is hardly possible. The diffusion and rotation of dioxyethylene on Cu(110) are hindered by barriers in the range from 0.69 to 1.62 eV with diffusion being less probable in the more stable $\text{O}_{sb}\text{-C}_{hl}\text{-O}_{sb}$ configuration of dioxyethylene. Interestingly, in both configurations, the diffusion barriers are larger than the formation energy of dioxyethylene on Cu(110) with respect to the free CO_2 and H_2 molecule.

In spite of the strong binding of formate to Cu(110), the diffusion of formate is hindered by relatively low activation barriers in the range from 0.14 to 0.67 eV. For both formate adsorption orientations, parallel and perpendicular to the close-packed rows, the diffusion in $[\bar{1}\bar{1}0]$ direction is hindered by smaller barriers, but in particular for the $\text{O}_t\text{-C}_{lb}\text{-O}_t$ configuration perpendicular to the rows of the (110) surface the diffusion barrier (0.14 eV) is so low that it is comparable to those of hydrogen diffusion. This means that formate can move rather fast along the $[\bar{1}\bar{1}0]$ direction, and this also explains why formate is difficult to image in STM experiments [36] because of its high mobility.

C. Reaction steps in the methanol oxidation

After identifying the stable reaction intermediates in the methanol oxidation on Cu(110), we have searched for the reaction paths connecting these reaction intermediates using the nudged elastic band method [25, 26]. In addition to the reaction steps already discussed in the introduction, we considered the following microscopic reactions:



The calculated activation barriers on Cu(110) and oxygen-covered Cu(110) are listed in Table III. In the presence of atomic oxygen, both the methanol decomposition (reaction (8)) as well as the dioxyethylene formation from formaldehyde (reaction (4)) occur spontaneously associated with a large energy gain. The initial configurations correspond to oxygen positioned at the pseudo fcc hollow site and methanol or formaldehyde, respectively, in their precursor state on the clean surface. After the oxygen-supported methanol decomposition, the produced methoxy and hydroxyl are located at the short bridge and the pseudo fcc hollow site in the same cell.

Cu(110)	Diffusion path	Direction	E_h (eV)
CH ₃ OH	$\text{O}_{sb}\text{-H}_{hl} \rightarrow \text{O}_{sb}\text{-H}_{hl}$	$[\bar{1}\bar{1}0]$	0.00
	$\text{O}_{sb}\text{-H}_{hl} \rightarrow \text{O}_{sb}\text{-H}_{hl}$	[001]	0.27
CH ₃ O	$\text{O}_{sb} \rightarrow \text{O}_{lb}$	CH ₃ rotation	0.48
	$\text{O}_{sb} \rightarrow \text{O}_{lb}$		0.46
	$\text{O}_{sb} \rightarrow \text{O}_{sb}$	$[\bar{1}\bar{1}0]$	0.08
H ₂ COO	$\text{O}_{sb}\text{-C}_{hl}\text{-O}_{sb} \rightarrow \text{O}_{sb}\text{-C}_{hl}\text{-O}_{sb}$	$[\bar{1}\bar{1}0]$	1.12
	$\text{O}_{sb}\text{-C}_{hl}\text{-O}_{sb} \rightarrow \text{O}_{sb}\text{-C}_{hl}\text{-O}_{sb}$	[001]	1.62
	$\text{O}_{sb}\text{-C}_{hl}\text{-O}_{sb} \rightarrow \text{O}_{lb}\text{-C}_{hl}\text{-O}_{lb}$	rotation	1.31
	$\text{O}_{lb}\text{-C}_{hl}\text{-O}_{lb} \rightarrow \text{O}_{lb}\text{-C}_{hl}\text{-O}_{lb}$	[001]	0.69
	$\text{O}_{lb}\text{-C}_{hl}\text{-O}_{lb} \rightarrow \text{O}_{lb}\text{-C}_{hl}\text{-O}_{lb}$	$[\bar{1}\bar{1}0]$	0.91
	$\text{O}_{lb}\text{-C}_{hl}\text{-O}_{lb} \rightarrow \text{O}_{sb}\text{-C}_{hl}\text{-O}_{sb}$	rotation	0.79
HCOO	$\text{O}_t\text{-C}_{sb}\text{-O}_t \rightarrow \text{O}_t\text{-C}_{sb}\text{-O}_t$	$[\bar{1}\bar{1}0]$	0.50
	$\text{O}_t\text{-C}_{sb}\text{-O}_t \rightarrow \text{O}_t\text{-C}_{sb}\text{-O}_t$	[001]	0.56
	$\text{O}_t\text{-C}_{lb}\text{-O}_t \rightarrow \text{O}_t\text{-C}_{lb}\text{-O}_t$	$[\bar{1}\bar{1}0]$	0.14
	$\text{O}_t\text{-C}_{lb}\text{-O}_t \rightarrow \text{O}_t\text{-C}_{lb}\text{-O}_t$	[001]	0.67
H	$\text{H}_{fcc} \rightarrow \text{H}_{lb} \rightarrow \text{H}_{fcc}$	$[\bar{1}\bar{1}0]$	0.17
	$\text{H}_{fcc} \rightarrow \text{H}_{sb} \rightarrow \text{H}_{fcc}$	[001]	0.04

TABLE II: Diffusion barriers (E_h) for various reaction intermediates on Cu(110).

Reaction	Configuration	E_b (eV)		ΔE (eV)	Active bond
		forward	backward		
Eq. (3)	$O_{sb} + O_{fcc} \rightarrow \text{physisorption} + OH_{fcc}$	0.56	0.30	+0.26	C-H
Eq. (4)	$\text{physisorption} + O_{fcc} \rightarrow O_{sb}-C_{hl}-O_{sb}$	0.00	1.76	-1.76	C-O
Eq. (8)	$O_{sb}-H_{hl} + O_{fcc} \rightarrow O_{sb} + OH_{fcc}$	0.00	1.32	-1.32	O-H
Eq. (9)	$O_{sb}-H_{hl} \rightarrow O_{sb} + H_{fcc}$	0.68	0.53	+0.15	O-H
Eq. (10)	$O_{sb} \rightarrow \text{physisorption} + H_{fcc}$	1.22	0.00	+1.22	C-H
Eq. (11)	$O_{sb}-C_{hl}-O_{sb} \rightarrow O_t-C_{lb}-O_t + H_{lb}$	0.71	0.95	-0.24	C-H
	$O_{lb}-C_{hl}-O_{lb} \rightarrow O_t-C_{sb}-O_t + H_{fcc}$	0.55	1.37	-0.84	C-H
Eq. (12)	$O_t-C_{lb}-O_t \rightarrow \text{physisorption} + H_{lb}$	1.56	0.88	+0.67	C-H
	$O_t-C_{sb}-O_t \rightarrow \text{physisorption} + H_{fcc}$	1.48	0.76	+0.72	C-H
Eq. (13)	$OH_{sb} + H_{fcc} \rightarrow \text{physisorption}$	0.79	0.74	+0.05	O-H
Eq. (14)	$H_2^b \rightarrow H_{fcc} + H_{fcc}$	0.60	0.65	-0.05	H-H
	$H_2^t \rightarrow H_{sb} + H_{sb}$	0.58	0.73	-0.15	H-H
	$H_2^{hl} \rightarrow H_{sb} + H_{sb}$	0.64	0.76	-0.12	H-H

TABLE III: Activation barriers (E_b) for various reaction steps in the methanol oxidation on Cu(110) calculated using the nudged elastic band method. The difference ΔE is defined as the energy difference between final and initial state, i.e., by $\Delta E = E_{\text{final}} - E_{\text{init}}$. ΔE does not include the energy cost or gain for the separation of the reaction intermediates to infinity.

In this configuration, the methoxy and hydroxyl still interact attractively which is reflected by the energy gain of 0.23 eV compared to infinitely separated methoxy and hydroxyl.

As already mentioned, the isolated oxygen atoms are more reactive than the terminal oxygen atoms at the edge of oxygen islands within the added row reconstruction. In fact, we find that both the methanol decomposition to methoxy as well as the formaldehyde conversion to dioxymethylene do not occur spontaneously at the terminal oxygen atoms. These atoms interact attractively with the molecules, but the interaction is not strong enough for non-activated bond-breaking.

According to TPD experiments [1], in the temperature range from 200 to 300 K methanol is converted to methoxy, and the produced hydrogen atoms are removed from the surface as water according to the following scheme,



The calculated barrier for the associative water desorption from adsorbed atomic hydrogen and hydroxyl (reaction (13)) is 0.79 eV. The reverse reaction (dissociative adsorption of water) is hindered by a barrier of 0.74 eV (see Table III). Considering the low adsorption energy of water on Cu(110) (-0.20 eV, see Table I), it is clear that water rather desorbs from the Cu(110) surface instead of decomposing into hydrogen and hydroxyl. The water desorption removes the hydrogen from the surface and thus prevents the associative methanol desorption (backward reaction of (9)). Thus methoxy stays on the surface and can decompose into hydrogen and formaldehyde in spite of the fact that the barrier for the recombinative desorption of methoxy with hydrogen is much smaller than for the methoxy decomposition which has been calculated to be 1.22 eV. It should be noted here that experiments suggest that the barrier should be only 0.92 eV [4]. Reasons for the discrepancy between theory and experiment will be discussed below.

This methoxy decomposition is essential for the partial oxidation of methanol in the intermediate temperature range from 300 to 420 K [5, 6]. Once formaldehyde is formed through the decomposition of methoxy, it immediately desorbs. The hydrogen atoms created by the decomposition of methoxy also desorb recombinatively either with methoxy as methanol or as molecular hydrogen. The branching ratio between the different desorption fluxes found in TPD experiments [1] is well-reproduced in kinetic Monte Carlo simulations if the experimentally derived barrier for the methoxy decomposition is used [7]. At approximately 400 K, all methoxy species are removed from the surface, and the partial oxidation process of methanol is terminated.

For the further reaction steps towards the total oxidation of methanol, the dioxymethylene formation is a key reaction step which then converts to formate. Zhou *et al.* recently observed in temperature programmed reaction (TPR) experiments [37, 38] that CO_2 is only formed during the heating but not during the cooling part of the temperature cycle. Moreover, Carley *et al.* demonstrated that the formate creation is sensitive to the heating rate; slower heating enhances the formate concentration [10]. These results indicate that formate and successively CO_2 are created under the condition that formaldehyde is present on the surface for a sufficiently long time.

According to our periodic DFT calculations, in the presence of isolated oxygen atoms formaldehyde converts spontaneously to dioxymethylene associated with a large energy gain of 1.76 eV. Previous DFT calculations using a hybrid functional to describe the formaldehyde conversion to dioxymethylene on Cu(111) within a cluster model have found a barrier of 0.37 eV [12]. Recall also that the terminal oxygen atoms are also not active with respect to the dioxymethylene formation, as mentioned above.

This shows that on Cu(110) the spontaneous dioxymethylene formation requires the presence of iso-

lated oxygen atoms. However, it is important to realize that the water desorption described above not only removes the hydrogen from the surface, but also any isolated oxygen atoms. And therefore all formaldehyde created from the decomposition of methoxy is immediately removed from the surface because of its small adsorption energies if no isolated oxygen atom is in its vicinity. This explains why on oxygen-precovered Cu(110) only small amounts of formate are created [11]. In contrast, when oxygen is co-dosed [11] or under steady-state conditions [29] there is considerable amount of formate present on the surface.

These observations suggest that under these conditions there is always a sufficient amount of transient isolated oxygen atoms before incorporation into the well-ordered $p(2 \times 1)$, and these isolated oxygen atom then can react with formaldehyde before it desorbs. Even if no oxygen is co-dosed, there is still a small amount of CO₂ production at oxygen-precovered surfaces [1]. The CO₂ formation can also be explained by the presence of these isolated oxygen atoms [11]: at higher temperatures, oxygen atoms are thermally evaporated from the edges of the $p(2 \times 1)$ oxygen islands leading to the existence of the highly reactive isolated oxygen atoms.

Nevertheless, we looked for another channel for the methoxy decomposition in the presence of isolated oxygen atoms. In our previous study [5] relevant for the case of low oxygen coverage, we had only considered the indirect promotion of the C-H bond scission by an adsorbed oxygen atom in a neighboring unit cell. The indirect interaction leads to a lowering of the decomposition barrier by 0.14 eV. Now we have additionally considered the influence of oxygen on the C-H bond scission when methoxy and oxygen are located in the same unit cell of the Cu(110) surface. There is a strong attraction between the methyl group of the methoxy and the adsorbed oxygen atom causing a bending of the methoxy. In this bend geometry, the C-H bond scission barrier is significantly reduced by 0.66 eV to a value of 0.56 eV.

This barrier is even lower than the H₂ desorption barrier of 0.65 eV. If this pathway was always active, then formaldehyde desorption would have been observed at much lower temperatures in TPD experiments. This reaction mechanism does therefore not seem to be operative under low oxygen concentrations, but only if there is a continuous supply of oxygen during the reaction. STM experiments have shown that the methoxy-covered regions of Cu(110) are well separated from oxygen islands [36]. And our previous DFT calculations confirmed that there is an energy cost of about 0.5 eV to insert an atomic oxygen into $c(2 \times 2)$ methoxy islands from the clean Cu area [5]. On the other hand, if a methoxy molecule is placed into the $Op(2 \times 1)/Cu(110)$ added-row reconstruction, the adsorption energy is only -1.81 eV which means that it is about 1 eV less stable than on clean Cu(110) (see Table I).

This separation between oxygen and methoxy is also confirmed in TPD experiments [4] which demonstrated

that under low oxygen coverage formaldehyde formation at 370 K is not influenced by remaining oxygen on the surface. Another reaction route would be the methoxy decomposition promoted by the presence of surface hydroxyl, but previous calculations have already shown that surface hydroxyl only leads to a moderate reduction of the C-H bond breaking barrier on Cu by 0.1 eV [39].

Thus the scenario of the dioxymethylene formation induced by the presence of isolated oxygen atoms seems to be the most realistic one. The decomposition of dioxymethylene to formate is sensitive to the orientation of O-C-O bond with barriers of 0.71 eV for the most stable $O_{sb}-C_{hl}-O_{sb}$ adsorption geometry and 0.55 eV for the less stable $O_{lb}-C_{hl}-O_{lb}$ geometry (see Table III). The oxygen positions are shifted from the bridge to the top positions upon the C-H bond scission. Interestingly, the decomposition barriers are lower than the diffusion and rotation barriers of dioxymethylene; thus the molecule is not mobile but rather decays. Our results are in good agreement with XPS experiments showing that dioxymethylene is a reaction intermediate of medium stability which decomposes to formate at the temperature of 230 K [13].

At temperatures above 420 K, the only remaining intermediate on Cu(110) is formate [13]. The formate decomposition to CO₂ (reaction (12)) which immediately desorbs is hindered by large barriers of 1.48 and 1.56 eV, similar to dioxymethylene depending on the O-C-O orientation. The hydrogen that is also produced in this reaction desorbs recombinatively, too, according to the reverse reaction of (14). The calculated barriers for formate are in good agreement with the measured barriers on Cu(110) of 1.38 [40], 1.50 eV [41]. The formate decomposition is also sensitive to the direction of the surface termination, the measured barriers being 1.12 and 1.17 eV on Cu(111) [41, 42] and 1.61 eV on Cu(100) [43]. Interestingly, the lowest barrier has been found on the closed packed (111) surface which often shows lower catalytic activities than the more open surfaces.

Based on the DFT calculations, we are able to construct a reaction scheme for the methanol oxidation on oxygen-covered Cu(110) that considers all species observed in TPD experiments. This scheme illustrating several possible reaction routes is shown in Fig. 4. For each reaction intermediate we have indicated possible processes and the associated barriers. The scheme is now complete enough to address the kinetics of the methanol oxidation using the DFT barriers to derive the microscopic reaction constants within transition state theory [44].

The different pathways leading either to the partial or the total oxidation of methanol on oxygen-covered Cu(110) are illustrated in Fig. 5. The diffusion barriers are not included. Initially, two methanol molecules are interacting with the surface within a $p(2 \times 2)O/Cu(110)$ geometry (Fig. 5a). Assuming a stoichiometry between methanol and oxygen of 2:1, all the surface oxygen atoms are consumed during the methanol decomposition to

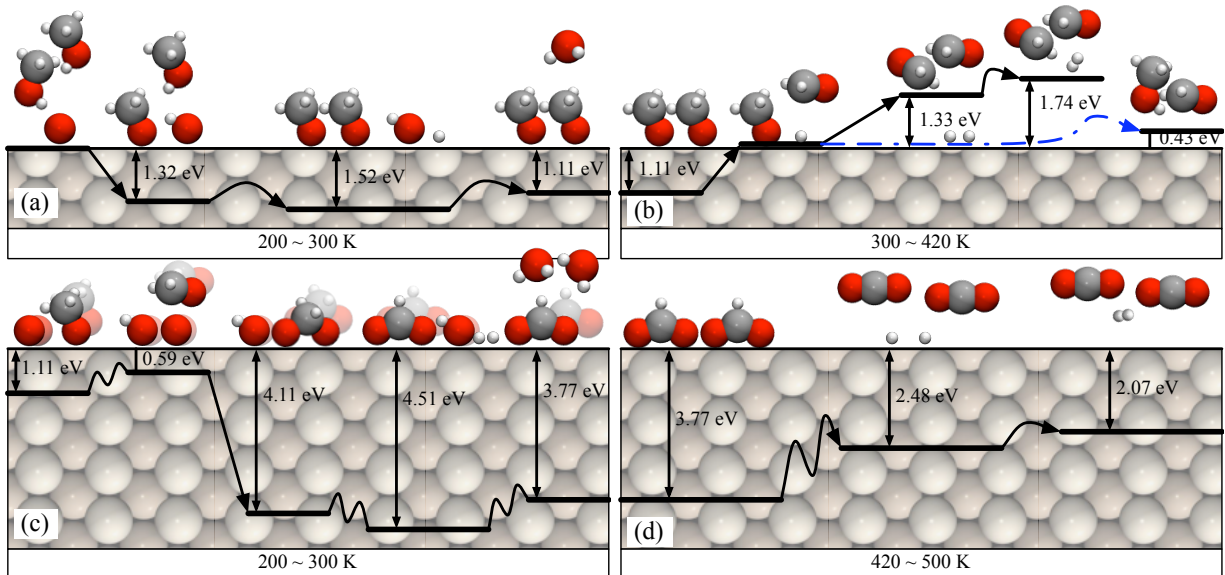


FIG. 5: The scenarios for the partial and the total oxidation of methanol on oxygen-covered Cu(110) with respect to the reference energy $E_{\text{ref}} = nE[\text{O}/\text{Cu}(110)] + 2E[\text{CH}_3\text{OH}^{(g)}]$. We assume that the oxygen atoms are initially located at the pseudo fcc hollow site within a $p(2 \times 2)$ periodicity. The methoxy and formate formation schemes are illustrated in panels (a) and (c), respectively. Panel (b) describes the final steps in the partial oxidation of methanol from methoxy to formaldehyde while panel (d) shows the corresponding final steps in the total oxidation from formate to CO_2 operative at higher temperatures.

close-shell molecules and metal substrates is usually underestimated in DFT. For the methoxy decomposition, the final state corresponds to physisorbed formaldehyde and atomic hydrogen on the surface. The calculated formaldehyde adsorption energy is -0.06 eV whereas the measured heat of desorption is 0.56 eV [1]. This underestimated physisorption energy of the products is particularly troublesome if the reaction barrier is located at a late position [56], i.e., if the transition state is located close to the final state. Then the underestimated binding energy of the final state will result in an overestimated barrier height. The methoxy decomposition corresponds to such reaction (see Fig. 6 of Ref. [5]). Thus it is well probable that the incorrect description of the van der Waals interaction causes the discrepancies in the barrier heights between theory and experiment. All the other barrier heights in the methanol oxidation calculated for processes that involve more strongly bound reactants as well as products seem to be well-described within DFT [7].

IV. CONCLUSIONS

We have performed periodic DFT calculations to address the methanol total oxidation path on Cu(110). The results of our calculations are in good agreement with the

experimentally found facts. The methanol oxidation corresponds to a rather complex process that is sensitive to the stoichiometry of the reactants, the structure of the surface and the temperature ramp in the experiments. We have particularly focused on the role of oxygen in the methanol oxidation. The selectivity for the partial and the total oxidation depends on the mixing ratio between methanol and oxygen. Low oxygen coverages promote the partial oxidation of methanol to formaldehyde by stabilizing the methoxy intermediate and removing hydrogen atoms from the surface via water desorption. The total oxidation, on the other hand, requires high oxygen concentrations on the surface. Under these conditions, the existence of isolated oxygen atoms lowers the methoxy decomposition barrier and promotes the conversion of formaldehyde to dioxymethylene which then easily decays to formate. The rate-limiting step in the total oxidation of methanol is then the formate decomposition into CO_2 and hydrogen.

Acknowledgments

This work has been supported by the German Science Foundation (DFG contract GR 1503/12-2) within the priority programme 1091 “Bridging the gap between ideal and real systems in heterogeneous catalysis”.

[1] Wachs, I. E.; Madix, R. J. *J. Catal.* **1978**, *53*, 208.

[2] Bowker, M.; Madix, R. J. *Surf. Sci.* **1980**, *95*, 190–206.

- [3] Greeley, J.; Mavrikakis, M. *J. Am. Chem. Soc.* **2004**, *126*, 3910.
- [4] Madix, R. J.; Telford, S. G. *Surf. Sci.* **1995**, *328*, L576–L581.
- [5] Sakong, S.; Groß, A. *J. Catal.* **2005**, *231*, 420–429.
- [6] Sakong, S.; Sendner, C.; Groß, A. *J. Mol. Struct. (Theochem)* **2006**, *771*, 117–122.
- [7] Sendner, C.; Sakong, S.; Groß, A. *Surf. Sci.* **2006**, *600*, 3258–3265.
- [8] Russell Jr., J. N.; Gates, S. M.; Yates Jr., J. T. *Surf. Sci.* **1985**, *163*, 516–540.
- [9] Sexton, B. A.; Hughes, A. E.; Avery, N. R. *Surf. Sci.* **1985**, *155*, 366–386.
- [10] Carley, A. F.; Davies, P. R.; Mariotti, G. G.; Read, S. *Surf. Sci.* **1996**, *364*, L525–L529.
- [11] Jones, A. H.; Poulston, S.; Bennett, R. A.; Bowker, M. *Surf. Sci.* **1997**, *380*, 31–44.
- [12] Gomes, J. R. B.; Gomes, J. A. N. F.; Illas, F. *J. Mol. Catal. A: Chem.* **2001**, *170*, 187–193.
- [13] Bowker, M.; Madix, R. J. *Surf. Sci.* **1981**, *102*, 542.
- [14] Poulston, S.; Jones, A. H.; Bennett, R. A.; Bowker, M. *J. Phys.: Condens. Matter* **1996**, *8*, L765–L771.
- [15] Jensen, F.; Bensenbacher, F.; Laesgaard, E.; Stensgaard, I. *Phys. Rev. B* **1990**, *41*, 10223.
- [16] Coulman, D. J.; Wintterlin, J.; Behm, R. J.; Ertl, G. *Phys. Rev. Lett.* **1990**, *64*, 1761.
- [17] Kern, K.; Niehus, H.; Schatz, A.; Zeppenfeld, P.; Goerge, J.; Comsa, G. *Phys. Rev. Lett.* **1991**, *67*, 855.
- [18] Bombis, C.; Moiseeva, M.; Ibach, H. *Phys. Rev. B* **2005**, *72*, 245408.
- [19] Bowker, M. *Top. Catal.* **1996**, *3*, 461–468.
- [20] Bowker, M.; Poulston, S.; Bennett, R. A.; Stone, P. J. *Phys.: Condens. Matter* **1998**, *10*, 7713.
- [21] Kresse, G.; Furthmüller, J. *Phys. Rev. B* **1996**, *54*, 11169.
- [22] Perdew, J. P.; Burke, K.; Ernzerhof, M. *Phys. Rev. Lett.* **1996**, *77*, 3865.
- [23] Blöchl, P. *Phys. Rev. B* **1994**, *50*, 17953–17979.
- [24] Kresse, G.; Joubert, D. *Phys. Rev. B* **1999**, *59*, 1758.
- [25] Henkelman, G.; Jónsson, H. *J. Chem. Phys.* **2000**, *113*, 9978.
- [26] Mills, G.; Jónsson, H. *Phys. Rev. Lett.* **1997**, *72*, 1124.
- [27] Vanderbilt, D. *Phys. Rev. B* **1990**, *41*, 7892.
- [28] Lischka, M.; Mosch, C.; Groß, A. *Electrochim. Acta* **2007**, *52*, 2219.
- [29] Günther, S.; Zhou, L.; Hävecker, M.; Knop-Gericke, A.; Kleimenov, E.; Schlögl, R.; Imbihl, R. **2006**, *125*, 114709.
- [30] Peremans, A.; Maseri, A. D. F.; Darville, J.; Gilles, J.-M.; Vigneron, J.-P. *Phys. Rev. B* **1999**, *45*, 8598–8609.
- [31] Leibsle, F. M.; Francis, S. M.; Haq, S.; Bowker, M. *Surf. Sci.* **1994**, *318*, 46–60.
- [32] Leibsle, F. M.; Francis, S. M.; Davis, R.; Xiang, N.; Haq, S.; Bowker, M. *Phys. Rev. Lett.* **1994**, *72*, 2569.
- [33] Sotiropoulos, A.; Milligan, P.; Cowie, B.; Kadodwala, M. *Surf. Sci.* **2000**, *444*, 52.
- [34] Groß, A. *Surf. Sci.* **2002**, *500*, 347–367.
- [35] Sakong, S.; Groß, A. *Surf. Sci.* **2003**, *525*, 107–118.
- [36] Silva, S. L.; Lemor, R. M.; Leibsle, F. M. *Surf. Sci.* **1999**, *421*, 135–145.
- [37] Zhou, L.; S. Günther, R. I. *J. Catal.* **2005**, *230*, 166–172.
- [38] Zhou, L.; S. Günther, R. I. *J. Catal.* **2005**, *232*, 295.
- [39] Gomes, J. R. B.; Gomes, J. A. N. F.; Illas, F. *Surf. Sci.* **1999**, *443*, 165–176.
- [40] Ying, D. H. S.; Madix, R. J. *J. Catal.* **1980**, *61*, 48–56.
- [41] Nakamura, I.; Nakano, H.; Fujitani, T.; Uchijima, T.; Nakamura, J. *J. Vac. Sci. Technol. A* **1999**, *17*, 1592–1595.
- [42] Nishimura, H.; Yatsu, T.; Fujitani, T.; Uchijima, T.; Nakamura, J. *J. Mol. Catal. A* **2000**, *135*, 3–11.
- [43] Taylor, P. A.; Rasmussen, P. B.; Ovesen, C. V.; Stoltze, P.; Chorkendorff, I. *Surf. Sci.* **1992**, *261*, 191–206.
- [44] Hänggi, P.; Talkner, P.; Borkovec, M. *Rev. Mod. Phys.* **1990**, *62*, 251.
- [45] Kratzer, P.; Hammer, B.; Nørskov, J. K. *J. Chem. Phys.* **1996**, *105*, 5595.
- [46] Greeley, J.; Mavrikakis, M. *J. Catal.* **2002**, *208*, 291–300.
- [47] Pallassana, V.; Neurock, M.; Lusvardi, V. S.; Lerour, J. J.; Kragten, D. D.; van Santen, R. A. *J. Phys. Chem. B* **2002**, *106*, 1656–1669.
- [48] Liu, Z.-P.; Hu, P. *J. Am. Chem. Soc.* **2003**, *125*, 1958–1967.
- [49] Knop-Gericke, A.; Hävecker, M.; Schedel-Niedrig, T.; Schlögl, R. *Top. Catal.* **2001**, *15*, 27.
- [50] Günter, M.; Ressler, T.; Bems, B.; Büscher, C.; Genger, T.; Hinrichsen, O.; Muhler, M.; Schlögl, R. *Catal. Lett.* **2001**, *71*, 37.
- [51] Mavrikakis, M.; Hammer, B.; Nørskov, J. K. *Phys. Rev. Lett.* **1998**, *81*, 2819.
- [52] Schlapka, A.; Lischka, M.; Groß, A.; Käsberger, U.; Jakob, P. *Phys. Rev. Lett.* **2003**, *91*, 016101.
- [53] Roudgar, A.; Groß, A. *J. Electroanal. Chem.* **2003**, *548*, 121.
- [54] Groß, A. *Top. Catal.* **2006**, *37*, 29.
- [55] Sauer, J.; Ugliengo, P.; Garrone, E.; Saunders, V. R. *Chem. Rev.* **1994**, *94*, 2095.
- [56] Groß, A. *Surf. Sci. Rep.* **1998**, *32*, 291–340.